1. INTRODUCTION

Polycyclic aromatic hydrocarbons (PAHs) compose a large group of organic compounds that consist of fused aromatic rings. They are emitted mainly from the incomplete combustion or pyrolysis of organic materials such as coal, oil, gas, waste, and biomass (Ravindra et al., 2008; Zhang and Tao, 2009). PAHs are the subject of considerable concern because of their potential risk to the environment and human health (Bhargava et al., 2004; Lai et al., 2017; Liu et al., 2017; Saha et al., 2017; Yang et al., 2017). As persistent semivolatile chemicals, PAHs can be transported over long distances to remote areas such as polar regions (Halsall et al., 2001; Huang et al., 2005) and high altitude regions such as the Tibetan Plateau (TP) (Chen et al., 2017; Wang et al., 2014).

The TP is one of the world's least scientifically studied regions in terms of PAH concentration, composition, transportation, source apportionment, and health risk assessment. Anthropogenic emissions within the TP are not of major concern compared with those in densely populated and industrialized parts of South and East Asia. Traditional agriculture and animal husbandry are the main economic pillars of the TP, whereas industry accounts for only 8% of the gross domestic product of this region (http://www.tibet.stats.gov.cn/). Therefore, the TP is considered a background site on a global scale. Numerous recent studies have reported atmospheric pollutants in this remote region (Cong et al., 2015; Li et al., 2016a; Lüthi et al., 2015); however, such studies have primarily been concerned with the role of the long-range transportation of pollutants emitted from South Asia. Notably, local anthropogenic activity in the TP contributes significantly to the atmospheric environment (Chen et al., 2015a; Gong et al., 2011; Li et al., 2012; Li et al., 2016a).

Lhasa, the provincial capital of Tibet, is currently undergoing rapid urbanization and

industrialization (Li and Wang, 2014; Li et al., 2016b; Ran et al., 2014). Previous studies have reported that the atmosphere in this high altitude city has been heavily influenced by local emissions (Cong et al., 2011; Huang et al., 2010; Li et al., 2016b). In addition, as the largest city in the TP, emissions from Lhasa are potential pollution sources to the surrounding areas (Li et al., 2008; Tao et al., 2010); for example, higher elemental and organochlorine pesticide concentrations were reported in aerosol samples from Lhasa than in those from more remote sites in the TP (Cong et al., 2011; Li et al., 2008). Current use and local emissions of organochlorine pesticides may contribute to environmental contamination in the populated agricultural Lhasa River Basin (Li et al., 2008). Radiocarbon isotope measurements of total carbon emissions revealed biomass burning and the incineration of agricultural waste, which contributed more to carbonaceous aerosols in winter than summer (Huang et al., 2010). Fine particulate matter ($PM_{2.5}$) in Lhasa is characterized by its low organic carbon to elemental carbon ratio, which reflects the heavy influence of vehicle emissions (Li et al., 2016b). Regarding PAHs, two studies have reported atmospheric PAH concentrations and compositions in Lhasa (Gong et al., 2011; Liu et al., 2013). Diagnostic ratios and principal component analysis revealed that atmospheric PAHs in Lhasa were primarily derived from local human activities such as vehicle emissions and incense burning. However, current knowledge of PAH source apportionment and its effects on the health of locals in Lhasa remains limited.

This paper presents the results of particulate-phase PAH observations in Lhasa during 2013 to 2014. The main objectives were as follows: (1) to investigate the atmospheric PAH concentrations and compositions in Lhasa; (2) to identify the seasonal variations of PAH concentrations and apportion the PAH sources by using a positive matrix factorization (PMF) model; and (3) to assess the health risks experienced due to PAHs in Lhasa.

2. METHODS

2.1 Sample collection

A total suspended particle (TSP) filter sampler (flow rate: 100 L min^{-1}; KC-120H, Qingdao Laoshan Applied Technology Institute, Qingdao, China) was placed on the rooftop (20 m above ground) of the Institute of Tibetan Plateau Research, Lhasa (E29.65°, N91.03°, 3642 m). A total of 62 samples were collected on prebaked quartz fiber filters (diameter: 90 mm; Whatman plc, Maidstone, United Kingdom) from April 2013 to March 2014 with duration of each sample as 24 h. TSP filter samples were collected continuously every week. For example, we collected 3 samples each week in spring but 1 sample in other seasons. However, several samples could not be collected due to lack of power or equipment breakdown in some periods. Finally, 19, 17, 11, and 15 samples were collected in spring, summer, autumn, and winter, respectively. All filters were prebaked at 550 °C for 6 h before sampling. They were equilibrated at constant temperature and humidity (25 ± 3 °C, 30 ± 5%) for 72 h and weighed using a microbalance with a sensitivity of ±0.01 mg before and after sampling. The volume of air passing through each filter was converted into standard atmospheric conditions (25 °C, 101.3 kPa). Ten field blank filters were collected once each month by placing in the sampler, which had no air drawn through it. And 3, 3, 2, and 2 blank filters were collected in spring, summer, autumn, and winter, respectively. Lhasa is a famous historic tourist city where considerable seasonal variations in traffic and religious activities occur. It exhibits the typical characteristics of four seasons, namely spring (March–May), summer (June–September), autumn (October–November), and winter (December–February). Meteorological parameters of studying period were recorded with automatic observation instruments at Lhasa Station. According to the observation, the air temperature ranged

from -5.7 to 21.2 °C with an average of 9.0 °C, and the relative humidity ranged from 7 to 75% with an average of 38.7% (Wan et al., 2016). The annual mean precipitation amount is around 400 mm with the majority of precipitation occurred frequently between June and September because of the summer monsoon activities, but it was relatively dry during spring and winter. The largest coal-fired power plant of Tibet (Dongga power plant) and the Dongga cement factory were located about 10 km west of our sampling site. In addition, our sampling site is close to Jinzhu road which is one of the busiest roads in Lhasa city with large numbers of trucks and other vehicles running. These are potential sources of particles in the atmosphere (Huang et al., 2013).

2.2 Extraction and analysis

Sonication extraction was used as detailed in Chen et al. (2015b). Here, the method is described briefly. A quarter of each filter was cut into pieces, placed into a glass tube, and immersed in 20 mL of dichloromethane (DCM) and *n*-hexane (1:1). The extraction was performed by sonication twice at 27 °C for 30 min. Every single sample was spiked with deuterated PAHs (naphthalene-d8, acenaphthene-d10, phenanthrene-d10, chrysene-d12, and perylene-d12) as recovery surrogates. The extracts were evaporated to about 0.5 mL with a rotary evaporator, and transferred to a multilayer column filled with 2 g of activated silica gel, 4 g of neutral alumina, and 1 cm of anhydrous Na_2SO_4 (pre-soaked in *n*-hexane). Then, the column was eluted by a mixture of 10 mL of *n*-hexane and 20 mL of DCM/*n*-hexane (1:1). The eluent solvent was blown down to a final volume of 1 mL under a gentle stream of nitrogen. Finally, the solution was transferred to a 1.5-mL vial and stored at -20 °C for rejection.

Sixteen PAHs (naphthalene (Nap), aecnaphthene (Ace), acenaphthylene (Aecl), anthracene (Ant), fluorene (Flu), phenanthrene (Phe), benzo(a)anthracene (BaA), chrysene (Chr), fluoranthene (Fla),

pyrene (Pyr), benzo(a)pyrene (BaP), benzo(b)fluoranthene (BbF), benzo(k)fluoranthene (BkF), dibenzo(a,h)anthracene (DahA), benzo(g,h,i)perylene (BghiP) and indeno(1,2,3-cd)pyrene (IndP)) prioritized by the United States Environmental Protection Agency (US EPA) were analyzed at the State Key Laboratory of Cryospheric Sciences, Chinese Academy of Sciences Northwest Institute of Eco-Environment and Resources, China, by using gas chromatography–mass spectrometry with a 30 × 250-μm ID HP-5MS. High-purity helium was used as a carrier gas at a constant flow rate of 1.0 mL min^{-1}. The mass spectrometer was operated in 70-Ev electron impact mode. The oven temperature was 100 °C, which was held stable for 2 min. Then it was ramped to the final temperature of 260 °C with different rate of increase; to 170 °C at 25 °C min^{-1}, to 225 °C at 8 °C min^{-1}, to 235 °C at 0.7 °C min^{-1}, to 260 °C at 25 °C min^{-1}, and finally held at 260 °C for 2 min. The temperature of the injector was 250 °C and that of the transfer line was 280 °C (Chen et al., 2017). Nap was not analyzed as it was detected with high concentration in the laboratory and field blanks.

2.3 Quality control

All analytic procedures were carried out using same method with strict quality assurance and control measures with Chen et al. (2017). Laboratory and field blanks were extracted and analyzed in the same way as the samples. The recoveries in field samples were 74-93%, 80-97%, 83-105%, and 89-109% for acenaphthene-d10, phenanthrene-d10, chrysene-d12, and perylene-d12 as inferred standards, respectively. The PAH concentrations were not corrected for the recoveries.

2.4 Gas/particle partitioning estimation

Octanol–air partition coefficient (K_{OA})-based model has been proved applicable to estimate the gas-particle partitioning of PAHs (Cheruiyot et al., 2015; Cheruiyot et al., 2016; Wang et al., 2018). The temperature–dependent K_{OA} values can be measured directly using the GC retention time method with an equation as Eq (1) (Harner and Bidleman, 1996):

$$\text{Log } K_{OA} = A + B/(T, K) \qquad (1)$$

The regression parameters (A and B) were given by Harner and Bidleman (1998) and Odabasi et al. (2006). The difference of K_{OA} values of PAHs among four seasons were calculated by adjusting the equations to the average ambient temperature (Pre-monsoon: 5 °C, Monsoon: 16 °C, Post-monsoon: 14 °C, and Winter: 1.5 °C) (Table 1). Then the gas-particle partition coefficient (K_P) can be predicted by equation (2) if the organic matter fraction *f*om of the aerosols are known and assuming that all of the particle organic matter is available to absorb gas-phase compounds.

$$\log K_P = \log K_{OA} + \log f\text{om} - 11.91 \qquad (2)$$

In this study, the average organic carbon concentrations were 13.2, 10.2, 30.6, and 35.9 μg/m^3 for these four seasons in aerosols of sampling site. And organic compounds contributed 18.3%, 16.9%, 25.7%, and 23.9% to total suspended particles in four seasons. Finally, we can estimate the gas phase PAHs using equation (3):

$$K_P = (C_p/C_{TSP})/C_g \qquad (3)$$

where C_p and C_g are the PAH concentrations in the particulate and gas phases, respectively, and C_{TSP} is the concentration of TSP in the air.

2.5 PMF receptor model

PMF is a powerful factorization method used to calculate the source profiles and contributions of pollutants in the environment. It has been used extensively for atmospheric source identification (Paatero and Tapper, 1994; Callén et al., 2014; Dvorská et al., 2012). PMF analysis is described in detail in Chen et al. (2016). A 62 × 15 (62 samples each containing 15 PAHs) dataset was input into the PMF 5.0 model to conduct source apportionment of atmospheric PAHs in Lhasa. A random seed mode and random starting point were selected. After testing three to six factors, a four-factor solution was adopted. Correlation indices between the estimated and measured concentrations ranged from 0.75 (Ace) to 0.92 (IcdP and BghiP), which suggested that the measured concentrations were fully explained by the four selected factors.

2.6 Cancer risk assessment

The carcinogenic potency of PAH exposure can be estimated as the sum of each individual BaP equivalent (BaP_{eq}) based on the toxic equivalency factor (TEF) of each individual PAH including both particle and gas phase PAHs (Nisbet and LaGoy, 1992; Petry et al., 1996; US EPA 2010). The TEF data in Nisbet and LaGoy (1999) were used in this study; BaP_{eq} was calculated as follows:

$$\text{Total } BaP_{eq} = \Sigma_i(C_i \times TEF_i) \qquad (1)$$

where C_i is the concentration of an individual PAH and TEF_i is its TEF. Inhalation was determined to be the main exposure pathway for PAHs in the air. We applied the following inhalation exposure assessment model recommended by the US EPA to calculate the daily exposure dose (DED) of BaP_{eq}:

$$\text{DED} = \frac{\text{C}\times\text{IR}\times\text{EF}\times\text{ED}}{\text{BW}\times\text{AT}} \times cf \qquad (2)$$

where DED is the DED of BaP_{eq} through the inhalation pathway (mg (kg day)$^{-1}$), C is the airborne BaP_{eq} concentration (ng m^{-3}), IR is the air inhalation rate (m^3 day^{-1}), EF is the exposure frequency (day year^{-1}), ED is the exposure duration (year), BW is the body weight (kg), AT is the averaging time (day), and *cf* is the conversion factor (in this study, $cf = 10^{-6}$).

The carcinogenic risk (CR) associated with inhalation exposure was calculated using Eq. (2), adapted from the US EPA (1989) and expressed as follows:

$$\text{CR} = \text{DED} \times \text{CSF} \times \left(\frac{\text{BW}}{70}\right)^{1/3} \qquad (3)$$

where CR is the probability of developing cancer over a lifetime because of exposure to atmospheric PAHs and CSF is the cancer slope factor, which quantitatively defines the relationship between carcinogen exposure dose and degree of CR. The CSFs used were derived assuming a body weight of 70 kg, which deviates from the actual conditions of the exposure populations of various age groups. Thus, the CSF values were extrapolated to actual body weights in various age groups by multiplying

the conversion factor $(BW/70)^{1/3}$, recommended by the US EPA (2004).

3. RESULTS AND DISCUSSION

3.1 PAH concentrations and compositions

During the study period, the particle phase PAH concentrations varied between 9.18 and 211 ng m^{-3} with an average of 45.0 ± 60.4 ng m^{-3} (Table 2). Although the annual average PAH concentration was considerably lower than those reported in numerous areas of northern China such as Shanxi, Shandong, and Beijing (Zhang et al., 2016) and South Asia such as Kathmandu (Chen et al., 2015) and Delhi (Sarkar and Khillare, 2013), it was higher than those observed at background sites in the TP. For example, PAHs in Lulang on the southeastern TP ranged from 0.06 to 2.53, with a mean value of 0.59 ng m^{-3} (Chen et al., 2014). In Zhongba and Nyalam, the mean PAH concentrations were 8.78 and 5.60 ng m^{-3}, respectively (Chen et al., 2017; Wang et al., 2014). This indicated that although the atmosphere in Lhasa is relatively clean compared to other Asian cities, it is affected by local anthropogenic activities. In addition, the PAH concentration had evidently increased since the two studies conducted in Lhasa in 2006 and 2007 (Table 2), implying that emissions might have increased as a result of urbanization (Gong et al., 2011; Liu et al., 2013).

Evident seasonal variations in the total PAH concentrations were observed, with the maximum and minimum concentrations occurring in winter and summer, respectively (Fig. 2). Based the Octanol–air partition coefficient (K_{OA}) model, the gas phase PAH concentrations were calculated, which also demonstrated clear seasonal variation with the highest concentrations occurred in summer, decreasing to minimum concentrations in winter (Table 3). Previous studies have reported that

seasonal variations of some atmospheric pollutants in Lhasa were mainly influenced by vehicle emissions in summer and biomass burning, power plants, and religious activities during the other seasons (Huang et al., 2010; Gong et al., 2011). During the cold season, biomass or coal combustion for heating increased as the temperature drops (Huang et al., 2010). And the incense burning in the temples for religious activities might be another important emission source of PAHs (Liu et al., 2013). Furthermore, low temperature (-7~9 °C) strengthens the condensation of gas phase PAHs onto atmospheric particles, leading to higher concentrations of particle phase PAHs in winter (Gong et al., 2011). A greater abundance of PAHs from late autumn to winter implied that PAH contributions from anthropogenic activities increase in the cold season, whereas in summer, although vehicle use and the frequency of tourist activities increase, high rainfall (approximately 70% of the total annual precipitation) washes most suspended particles and particle-bound pollutants out of the atmosphere (Cong et al., 2011; Wan et al., 2016). In addition, the high summer temperature (9~22 °C) enhances the evaporation of particle-phase to gas-phase PAHs, which leads to lower PAH concentrations in summer (Liu et al., 2017; Tham et al., 2008); for example, the contribution of PAHs with low molecular weights (e.g., Ace, Acel, Ant, Flu, and Phe) was twice as high in winter than in summer, indicating that temperature is a crucial factor possibly resulting in seasonal variations between PAH concentrations.

According to the number of aromatic rings, the aforementioned 15 PAHs were classified into four groups: three-ring (Acel, Ace, Flu, Phe, and Ant), four-ring (Fla, Pry, BaA, and Chr), five-ring (BbF, BkF, BaP, and DahA), and six-ring (IndP and BghiP) PAHs (Kaur et al., 2013). The seasonal composition patterns of the particle phase 15 PAHs over four seasons are shown in Fig. 3; four- and five-ring PAHs contributed the most, followed by six- and three-ring PAHs. Correspondingly, gas

phase PAHs showed different composition patterns with three-ring compounds especially Aec, Acel, and Flu contributed most to the total particles (Table 3). However, the profiles of particle phase PAHs in Lhasa varied across all four seasons; for example, the contributions of four-ring PAHs were highest in winter at 56.5%, which decreased to 31.5% in summer. By contrast, the contributions of five- and six-ring PAHs exhibited the opposing trend. Previous studies have reported that coal combustion and biomass burning release an abundance of four-ring PAHs, whereas five- and six-ring PAHs mainly originate from high-temperature combustion processes such as vehicle exhausts (Dachs et al., 2000; Moon et al., 2008). The variations in PAH compositions evidently reflect the aforementioned changes in source contributions during the sampling period (Huang et al., 2010; Gong et al., 2011). Meanwhile, the partitioning of PAH between particle- and gas-phase is temperature sensitive and consequently four-ring compounds making an apparently greater contribution in winter as opposed to summer.

3.2 PAH sources assessed by diagnostic ratios

Diagnostic ratios are used frequently to identify PAH origins (Rajput et al., 2014; Yunker et al., 2002). In this study, IndP/(IndP + BghiP) and Fla/(Fla + Pyr) ratios were used simultaneously to cross-check the results and reduce uncertainty. The IndP/(IndP + BghiP) ratios were below 0.5 in all seasons, implying a strong contribution from petroleum combustion (Table 4). The mean Fla/(Fla + Pyr) ratios were 0.54 ± 0.03, 0.48 ± 0.02, 0.49 ± 0.02, and 0.52 ± 0.03 in spring, summer, autumn, and winter, respectively, with lower values in summer and autumn, thereby reflecting the impact of vehicles as PAH sources (Table 4). The tourist activities mainly happen from May to October especially in summer. And vehicle emission is higher during this period than the cold season. Higher values were observed in winter and spring, implying that the biomass contribution increased in these

seasons because of low temperatures. Biomass energy consumption was considered as the largest parts (about 40%) of total energy consumption, compared to coal and liquid fossil fuel, 5% and 16%, respectively (Hua, 2009). These results are consistent with those of the PMF model in Subsection 3.3.

3.3 Source apportionment of all PAHs determined using PMF

Fig. 4 shows the four source contributions of all samples and PMF factors of all profiles and contributions. Each column corresponds to the concentration profile of one PAH. The first factor accounted for 9.30% of all PAHs. The profile contains more volatile PAHs, which are similar to those reported as air–ground and air–soil emissions (Cheng et al., 2012; Nelson et al., 1998). Accordingly, the first factor was classified as air–surface exchange. The second factor accounted for 14.3% of all PAHs and showed high loadings of Fla and Pyr, which are typical markers of coal combustion (Huang et al., 2010; Qin et al., 2014). Thus, this factor was classified as coal emission. The third factor accounted for 48.4% of all PAHs and had high loadings of four-ring PAHs such as Fla, Pyr, and Chr and moderate contributions from BaA, Bbf, Bkf, and Bap. This type of profile is mainly the result of biomass burning (Lin et al., 2011; Wang et al., 2015). In Lhasa, biomass varieties such as wood and yak dung are burned year-round for heating and cooking, especially in winter (Huang et al., 2010). Thus, this factor was assigned as biomass burning. The fourth factor contributed 27.9% of all PAHs. High loadings of five- and six-ring PAHs were observed. IndP and BghiP are typical markers of traffic emissions (Simcik et al., 1999) and IndP is associated with diesel emissions (Li and Kamens, 1993). A similar profile was observed in aerosols at a site downwind of East Asia (Wang et al., 2014). As a famous tourist city, Lhasa has undergone a rapid increase in vehicle use in recent years, especially in summer and autumn. Therefore, this factor was deemed to

be caused by vehicle emissions.

In summary, the main source of atmospheric PAHs in Lhasa is biomass combustion, followed by vehicle emissions, coal combustion, and air–surface exchange. However, notably, determining precise source contributions based on the PMF model and diagnostic ratios only is difficult because of high uncertainty. In addition, the PAH source profiles for coal combustion and residential biomass combustion are usually similar, thereby engendering difficulties in separating these two factors. Thus, further research integrating other methods or evidence is required.

3.4 Health risk values

The BaPeq values for particle phase PAHs during the sampling period varied from 1.48 to 24.5 ng m^{-3} with an average of 6.27 ± 8.55 ng m^{-3}. For gas phase PAHs, the BaPeq values were 4.28, 11.6, 6.23, and 3.64 ng m^{-3} for spring, summer, autumn, and winter, respectively with an similar average value (6.43± 4.15 ng m^{-3}) with particle phase PAHs. The most recent ambient air quality standard for China (GB3095-2012) showed an improvement in the limited value of atmospheric BaP from 10 to 1 ng m^{-3}. All BaP_{eq} concentrations calculated in Lhasa were higher than the limit value, which indicates the potential for adverse health effects caused by atmospheric PAHs in this region.

People of three age groups (children, teenagers, and adults) were examined to effectively estimate the exposure levels of BaP_{eq} in various age ranges. Table 5 shows the parameters of these three age groups used in the exposure assessment. Based on the data, the DEDs and CR of BaP_{eq} in Lhasa were characterized for all three age groups. The CRs of particle phase PAHs were estimated as 9.20×10^{-7}, 7.20×10^{-7}, and 2.84×10^{-6} for children, teens, and adults, respectively. While for gas phase PAHs, the CRs were similar with particle phase PAHs for three groups, with values as 9.43×10^{-7}, 7.38×10^{-7}, and 2.91×10^{-6}. The CR values of total (gas and particle phase) PAHs were 1.86 ×

313 10^{-6}, 1.46 × 10^{-6}, and 5.76 × 10^{-6}, respectively, which were one time higher than those of particle
314 phase PAHs. PAHs are present in the atmosphere in both particle and gas phases. In this study, the
315 calculated gas phase PAH concentrations were much higher than those of particle phase. And CR
316 values doubled after adding gas phase PAHs. Therefore, additional detailed surveys of gas phase
317 PAHs should be considered in further study. Most regulatory programs employ a limiting CR value
318 of 1.00E−05 (De Miguel et al., 2007). The lifetime CR (LCR) in Lhasa was determined by
319 calculating the CR values of two types of PAHs for all three age groups. The results showed that the
320 LCR (9.08 × 10^{-6}) was lower than the acceptable target risk value, indicating that atmospheric PAHs
321 in Lhasa pose no or little potential CR to locals.
322
323 **4. CONCLUSION**
324
325 PAH concentrations in Lhasa were higher than those in other remote sites in the TP, indicating
326 that the atmospheric environment in Lhasa has been influenced by local anthropogenic activities.
327 Clear seasonal variations of PAH concentrations were observed, with maximum and minimum
328 values occurred in winter and summer, respectively. Gas phase PAH concentrations were much
329 higher than particle phase PAHs and have opposite seasonal trends. Particle phase PAH profiles,
330 especially those of four-ring compounds, changed significantly between winter and summer, thereby
331 reflecting the variations in emission sources in different seasons. However, three-ring species
332 especially Ace, Acel, and Flu contributed most to gas phase PAHs. The particle phase PAH sources
333 were quantified using the PMF model and the results revealed that atmospheric PAHs in Lhasa
334 originated mainly from the combustion of biomass fuels (48.4%) and vehicle emissions (27.9%). The
335 diagnostic molecular ratios provided similar results. The average BaP_{eq} of the PAHs was higher than

the new limit value in China, thereby indicating the potential for adverse health effects on locals. And a probabilistic health risk assessment showed that atmospheric PAHs in Lhasa posed no or little CR for locals.

ACKNOWLEDGEMENTS

This study is supported by the National Natural Science Foundation of China (41705132, 41630754, 41675130), State Key Laboratory of Cryosphere Science (SKLCS-OP-2018-01) and Chinese Academy of Sciences (QYZDJ-SSW-DQC039). The authors acknowledge Xi Luo for collecting the samples. The manuscript was edited by Wallace Academic Editing.

REFERENCES

Bari, M., Baumbach, G., Brodbeck, J., Struschka, M., Kuch, B., Dreher, W., Scheffknecht, G. (2011). Characterisation of particulates and carcinogenic polycyclic aromatic hydrocarbons in wintertime wood-fired heating in residential areas. Atmos. Environ. 45: 7627–7634.

Bhargava, A., Khanna, R., Bhargava, S., Kumar, S. (2004). Exposure risk to carcinogenic PAHs in indoor-air during biomass combustion whilst cooking in rural India. Atmos. Environ. 38: 4761–4767.

Callén, M., Iturmendi, M., López, J. (2014). Source apportionment of atmospheric $PM_{2.5}$-bound polycyclic aromatic hydrocarbons by a PMF receptor model. Assessment of potential risk for human health. Environ. Pollut. 195: 167–177.

Cheng, H., Deng, Z., Chakraborty, P., Liu, D., Zhang, R., Xu, Y., Luo, C., Zhang, G., Li, J. (2013). A comparison study of atmospheric polycyclic aromatic hydrocarbons in three Indian cities using PUF disk passive air samples. Atmos. Environ. 73: 16–21.

359 Chen, P., Kang, S., Bai, J., Sillanpää, M., Li, C. (2015a). Yak dung combustion aerosols in the
360 Tibetan Plateau: Chemical characteristics and influence on the local atmospheric environment.
361 Atmos. Res. 156: 58–66.
362 Chen, P., Kang, S., Li, C., Rupakheti, M., Yan, F., Li, Q., Ji, Z., Zhang, Q., Luo, W., Sillanpää, M.
363 (2015b). Characteristics and sources of polycyclic aromatic hydrocarbons in atmospheric aerosols in
364 the Kathmandu Valley, Nepal. Sci. Total Environ. 538: 86–92.
365 Chen, P., Li, C., Kang, S., Rupakheti, M., Panday, A., Yan, F., Li, Q., Zhang, Q., Guo, J., Ji, Z.,
366 Rupakheti, D., Luo, W. (2017). Characteristics of particulate-phase polycyclic aromatic
367 hydrocarbons (PAHs) in the atmosphere over the central Himalayas. Aerosol Air Qual. Res. 17:
368 2942–2954.
369 Chen, S., Liao, C. (2006). Health risk assessment on human exposed to environmental polycyclic
370 aromatic hydrocarbons pollution sources. Sci. Total Environ. 366: 112–123.
371 Chen, Y., Cao, J., Zhao, J., Xu, H., Arimoto, R., Wang, G., Han, Y., Shen, Z., Li, G. (2014).
372 n-Alkanes and polycyclic aromatic hydrocarbons in total suspended particulates from the
373 southeastren Tibetan Plateau: concentrations, seasonal variations, and sources. Sci. Total Environ.
374 470: 9–18.
375 Cheruiyot, N.K., Lee, W.J., Mwangi, J.K., Wang, L.C., Lin, N.H., Lin, Y.C., Cao, J., Zhang, R. and
376 Chang-Chien, G.P. (2015). An overview: Polycyclic aromatic hydrocarbon emissions from the
377 stationary and mobile sources and in the ambient air. Aerosol Air Qual. Res. 15: 2730–2762.
378 Cheruiyot, N.K., Lee, W.J., Yan, P., Mwangi, J.K., Wang, L.C., Gao, X., Lin, N.H. and Chang-Chien,
379 G.P. (2016). An Overview of PCDD/F Inventories and Emission Factors from Stationary and Mobile
380 Sources: What We Know and What is Missing. Aerosol Air Qual. Res. 16: 2965–2988.

Cong, Z., Kang, S., Kawamura, K., Liu, B., Wan, X., Wang, Z., Gao, S., Fu, P. (2015). Carbonaceous aerosols on the south edge of the Tibetan Plateau: concentrations, seasonality and sources. Atmos. Chem. Phys. 15: 1573–1584.

Cong, Z., Kang, S., Luo, C., Li, Q., Huang, J., Gao, S., Li, X. (2011). Trace elements and lead isotopic composition of PM10 in Lhasa, Tibet. Atmos. Environ. 45: 6210–6215.

Dachs, J., Eisenreich, S. (2000). Adsorption onto aerosol soot carbon dominates gas-particle partitioning of polycyclic aromatic hydrocarbons. Environ. Sci. Technol. 34: 3690–3697.

Dvorská, A., Komprdová, K., Lammel, G., Klánová, J., Helena, P. (2012). Polycyclic aromatic hydrocarbons in background air in central Europe-seasonal levels and limitations for source apportionment. Atmos. Environ. 46: 147–154.

Grimmer, G., Jacob, J., Naujack, K. (1983). Profile of the polycyclic aromatic compounds from crude oils. Fresenius Zeitschrift Fur Analytische Chemie. 314: 29–36.

Gong, P., Wang, X., Yao, T. (2011). Ambient distribution of particulate-and gas-phase n-alkanes and polycyclic aromatic hydrocarbons in the Tibetan Plateau. Environ. Earth. Sci. 64: 1703–1711.

Halsall, C., Sweetman, A., Barrie, L., Jones, K. (2001). Modelling the behaviour of PAHs during atmospheric transport form the UK to the Arctic. Atmos. Environ. 35: 255–267.

Harner T, Bidleman T. (1996). Measurements of octanol-air partition coefficients for polychlorinated biphenyls. J Chem Eng Data. 41: 895–899.

Harner T, Bidleman T. (1998). Octanol-air partition coefficient for describing particle/gas partitioning of aromatic compounds in urban air. Environ Sci Technol. 32: 1497–1502.

Hua, H.(2009). The research on the usage of energy in Lhasa area. Energy Res. Util. 30–32 (In Chinese).

Huang, H., Blanchard, P., Halsall, C., Bidleman, T., Stem, G., Fellin, P., Muir, D., Barrie, L., Jantunen, L., Helm, P., Ma, J., Konoplev, A. (2005). Temporal and spatial variabilities of atmospehric polychlorinated biphenyls (PCBs), organochlorine (OC) pesticides and polycyclic aromatic hydrocarbons (PAHs) in the Canadian Arctic: Results from a decade of monitoring. Sci. Total Environ. 342: 119–144.

Huang, J., Kang, S., Shen, C., Cong, Z., Liu, K., Wang, W., Liu, L. (2010). Seasonal variations and sources of ambient fossil and biogenic-derived carbonaceous aerosols based on ^{14}C measurements in Lhasa, Tibet. Atmos. Res. 96: 553–559.

Huang, J., Kang, S., Wang, S., Wang, L., Zhang, Q., Guo, J., Wang, K., Zhang, G., Tripathee, L. (2013). Wet deposition of mercury at Lhasa, the capital city of Tibet. Sci. Total Environ. 447: 123–132.

Kaur, S., Senthilkumar, K., Verma, V., Kumar, B., Kumar, S., Katnoria, J., Sharma, C. (2013). Preliminary Analysis of Polycyclic Aromatic Hydrocarbons in Air Particles (PM_{10}) in Amritsar, India: Sources, Apportionment, and Possible Risk Implications to Humans. Arch. Environ. Con. Tox. 65: 382–395.

Lai, Y., Tsai, C., Liang, Y., Chien, G. (2017). Distribution and sources of atmospheric polycyclic aromatic hydrocarbons at an industrial region in Kaohsiung, Taiwan. Aerosol Air Qual. Res. 17: 776-787.

Li, C., Bosch, C., Kang, S., Andersson, A., Chen, P., Zhang, Q., Cong, Z., Chen, B., Qin, D., Gustafsson, Ö. (2016a). Sources of black carbon to the Himalayan-Tibetan Plateau glaciers. Nat. Commun.7: 12574.

Li, C., Chen, P., Kang, S., Yan, F., Hu, Z., Qu, B., Sillanpää, M. (2016b). Concentrations and light

425 absorption characteristics of carbonaceous aerosol in $PM_{2.5}$ and PM_{10} of Lhasa city, the Tibetan
426 Plateau. Atmos. Environ. 127: 340–346.
427 Li, C., Kamens, R. (1993). The use of polycyclic aromatic hydrocarbons as source signatures in
428 receptor modelling. Atmos. Environ. 27: 523–532.
429 Li, C., Kang, S., Chen, P., Zhang, Q., Fang, G. (2012). Characterizations of particle-bound trace
430 metals and polycyclic aromatic hydrocarbons (PAHs) within Tibetan tents of south Tibetan Plateau,
431 China. Environ. Sci. Pollut. Res. 19: 1620–1628.
432 Li, J., Lin, T., Qi, S., Zhang, G., Liu, X., Li, K. (2008). Evidence of local emission of organochlorine
433 pesticides in the Tibetan plateau. Atmos. Environ. 42: 7397–7404.
434 Li, Q., Wang, C. (2014). Research on Urbanization in Tibet and its Environmental Impact. Chinese
435 Soft Science Magazine, pp:70–78 (in Chinese).
436 Lin, T., Hu, L., Guo, Z., Qin, Y., Yang, Z., Zhang, G., Zheng, M. (2011). Sources of polycyclic
437 aromatic hydrocarbons to sediments of the Bohai and Yellow Seas in East Asia. J. Geophy. Res.
438 Atmos. 116: D23305.
439 Liu, J., Li, J., Lin, T., Liu, D., Xu, Y., Chaemfa, C., Qi, S., Liu, F., Zhang, G. (2013). Diurnal and
440 nocturnal variations of PAHs in the Lhasa atmosphere, Tibetan Plateau: Implication for local sources
441 and the impact of atmospheric degradation processing. Atmos. Res. 124: 34–43.
442 Liu, J., Wang, Y., Li, P., Shou, Y., Li, T., Yang, M., Wang, L., Yue, J., Yi, X., Guo, L. (2017).
443 Polycyclic aromatic hydrocarbons (PAHs) at high mountain site in north China: Concentration,
444 source and health risk assessment. Aerosol Air Qual. Res. 17: 2867–2877.
445 Liu, X., Li, C., Tu, H., Wu, Y., Ying, C., Huang, Q., Wu, S., Xie, Q., Yuan, Z., Lu, Y. (2017). Analysis
446 of the effect of meteorological factors on $PM_{2.5}$-associated PAHs during autumn-winter in urban

447 Nanchang. Aerosol Air Qual. Res. 17: 3222–3229.
448 Lüthi, Z., Škerlak, B., Kim, S., Lauer, A., Mues, A., Rupakheti, M., Kang, S. (2015). Atmospheric
449 brown clouds reach the Tibetan Plateau by crossing the Himalayas. Atmos. Chem. Phys. 15: 1–15.
450 Moon, K., Han, J., Ghim, Y., Kim, Y. (2008). Source apportionment of fine carbonaceous particles by
451 positive matrix factorization at Gosan backgroud site in East Asia. Environ. Int. 34: 654–664.
452 Nelson, E., McConnell, L., Baker, J. (1998). Diffusive exchange of gaseous polycyclic aromatic
453 hydrocarbons and polychlorinated biphenyls across the air-water interface of the Chesapeake Bay.
454 Environ. Sci. Technol. 32: 912–919.
455 Nisbet, I., LaGoy, P. (1992). Toxic equivalency factors (TEFs) for polycyclic aromatic hydrocarbons
456 (PAHs). Regul. Toxicol. Pharm. 16: 290–300.
457 Odabasi M, Cetin E, Sofuoglu A. (2006). Determination of octanol-air partition coefficients and
458 supercooled liquid vapor pressures of PAHs as a function of temperature: Application to gas-particle
459 partitioning in an urban atmosphere. Atmos. Environ. 40: 6615–6625.
460 Paatero, P., Tapper, U. (1994). Positive matrix factorization: a non-negative factor model with
461 optimal utilization of error estimates of dara values. Environ. Metrics. 5: 111–126.
462 Petry, T., Schmid, P., Schlatter, C. (1996). The use of toxic equivalency factors in assessing
463 occupational and environmental health risk associated with exposure to airborne mixtures of
464 polycyclic aromatic hydrocarbons (PAHs). Chemosphere. 32: 639–648.
465 Qin, L., Han, J., He, X., Lu, Q. (2014). The emission characteristic of PAHs during coal combustion
466 in a fluidized bed combustor. Energy. Source. Part A. 36: 212–221.
467 Rajput, P., Sarin, M., Sharma, D., Singh, D. (2014). Atmospheric polycyclic aromatic hydrocarbons
468 and isomer ratios as tracers of biomass burning emissions in Northern India. Environ. Sci. Poll. Res.

21: 5724–5729.

Ran, L., Lin, W.L., Deji, Y.Z., La, B., Tsering, P.., Xu, B.Q., Wang, W. (2014). Source gas pollutants in Lhasa, a highland city of Tibet-current levels and pollution implications. Atmos. Chem. Phys. 14: 10721-10730.

Ravindra, K., Sokhi, R., Van Gridken, R. (2008). Atmospheric polycyclic aromatic hydrocarbons: Source attribution, emission factors and regulation. Atmos. Environ. 42: 2895–2921.

Sarkar, S., Khillare, P. (2013). Profile of PAHs in the inhalable particulate fraction: source apportionment and associated health risks in a tropical megacity. Environ. Monit. Assess. 185: 1199–1213.

Saha, M., Maharana, D., Kurumisawa, R., Takada, H., Yeo, B., Rodrigues, A., Bhattacharya, B., Kumata, H., Okuda, T., He, K., Ma, Y., Nakajima, F., Zakaria, M., Giang, D., Viet, P. (2017). Seasonal trends of atmospheric PAHs in five Asian megacities and source detection using suitable biomarkers. Aerosol Air Qual. Res. 17: 2247–2262.

Sicre, M., Marty, J., Saliot, A., Aparicio, X., Grimalt, J., Albaiges, J. (1987). Aliphatic and aromatic hydrocarbons in different sized aerosols over the Mediterranean Sea: occurrence and origin. Atmos. Environ. 21: 2247–2259.

Tang, N., Hattori, T., Taga, R., Igarashi, K., Yang, X., Tamura, K., Kakimoto, H., Mishukov, V., Toriba, A., Kizu, R. (2005). Polycyclic aromatic hydrocarbons and nitropolycyclic aromatic hydrocarbons in urban air particulates and their relationship to emission sources in the Pan–Japan Sea countries. Atmos. Environ. 39: 5817–5826.

Tao, S., Wang, W., Liu, W., Zuo, Q., Wang, X., Wang, R., Wang, B., Shen, G., Yang, Y., He, J. (2010). Polycyclic aromatic hydrocarbons and organochlorine pesticides in surface soils from the

491 Qinghai-Tibetan plateau. J. Environ. Monit. 13: 175–181.
492 Tham, Y., Takeda, K., Sakugawa, H. (2008). Polycyclic aromatic hydrocarbons (PAHs) associated
493 with atmospheric particles in Higashi Hiroshima, Japan: Influence of meteorological conditions and
494 seasonal variations. Atmos. Res. 88: 224–233.
495 Tsapakis, M., Stephanou, E. (2003). Collection of gas and particle semi-volatile organic compounds:
496 use of an oxidant denuder to minimize polycyclic aromatic hydrocarbons degradation during
497 high-volume air sampling. Atmos. Environ. 37: 4935–4944.
498 USEPA. (1989). Risk assessment guidance for superfund volume I human health evaluation manual
499 (part A). EPA/540/1-89/002. http://www.epa.gov/oswer/riskassessment/ragsa/pdf/rags-vol1-pta_
500 complete.pdf
501 USEPA. (2004). Risk assessment guidance for superfund volume I: human health evaluation manual
502 (part E, supplemental guidance for dermal risk assessment). EPA/540/R/99/005. http://www.epa.
503 gov/superfund/programs/risk/ragse/index.htm
504 Wan, X., Kang, S., Xin, J., Liu, B., Wen, T., Wang, P., Wang, Y., Cong, Z. (2016). Chemical
505 composition of size-segregated aerosols in Lhasa city, Tibetan Plateau. Atmos. Res. 174: 142–150.
506 Wang, C., Wang, X., Gong, P., Yao, T. (2014). Polycyclic aromatic hydrocarbons in surface soil
507 across the Tibetan Plateau: Spatial distribution, source and airesoil exchange. Environ. Pollut. 184:
508 138–144.
509 Wang, F., Lin, T., Feng, J., Fu, H., Guo, Z. (2015). Source apportionment of polycyclic aromatic
510 hydrocarbons in PM2.5 using positive matrix factorization modeling in Shanghai, China. Environ.
511 Sci. Proc. Impacts. 17: 197–205.
512 Wang, W., Cui, K., Zhao, R., Zhu, J., Huang, Q. and Lee, W.J. (2018). Sensitivity Analysis of

PM2.5-Bound Total PCDD/Fs-TEQ Content: In the Case of Wuhu City, China. Aerosol Air Qual. Res. 18: 407-420.

Yang, T., Hsu, C., Chen, Y., Young, L., Huang, C., Ku, C. (2017). Chatacterisitics, sources, and health risks of atmospheric $PM_{2.5}$-bound polycyclic aromatic hydrocarbons in Hsinchu, Taiwan. Aerosol Air Qual. Res. 17: 563–573.

Yunker, M., Macdonald, R., Vingarzan, R., Mitchell, R., Goyette, D., Sylvestre, S. (2002). PAHs in the Fraser River basin: a critical appraisal of PAH ratios as indicators of PAH source and composition. Org. Geochem. 33: 489–515.

Zhang, Y., Lin, Y., Cai, J., Liu, Y., Hong, L., Qin, M., Zhao, Y., Ma, J., Wang, X., Zhu, T., Qiu, X., Zheng, M. (2016). Atmospheric PAHs in North China: Spatial distribution and sources. Sci. Total Environ. 565: 994–1000.

Zhang, Y., Tao, S. (2009). Global atmospheric emission inventory of polycyclic aromatic hydrocarbons (PAHs) for 2004. Atmos. Environ. 43: 812–819.

538 Table 1 Parameters of equation (1) and octanol-air partition coefficients (K_{OA}) for PAHs at 5 ^{o}C, 16
539 ^{o}C, 14 ^{o}C and 1.5 ^{o}C in spring, summer, autumn and winter, respectively.
540

SN	PAH	A	B	Log K_{OA} (5 °C)	Log K_{OA} (16 °C)	Log K_{OA} (14 °C)	Log K_{OA} (1.5 °C)
1	Ace[b]	-2.20	2597	7.14	6.78	6.84	7.22
2	Acel[b]	-1.97	2476	6.93	6.59	6.65	7.01
3	Ant[b]	-3.41	3316	8.51	8.06	8.14	8.62
4	Flu[a]	-7.74	4332	7.58	7.19	7.26	7.67
5	Phe[a]	-5.62	3942	8.47	8.02	8.10	8.58
6	BaA[b]	-5.64	4746	11.4	10.7	10.8	11.5
7	Chr[b]	-5.65	4754	11.5	10.8	10.9	11.6
8	Fla[a]	-5.94	4417	9.70	9.16	9.26	9.83
9	Pyr[a]	-4.56	3985	9.77	9.22	9.32	9.90
10	BaP[b]	-6.50	5382	12.8	12.1	12.2	13.0
11	BbF[b]	-6.40	5285	12.6	11.8	12.0	12.7
12	BkF[b]	-6.42	5301	12.6	11.9	12.1	12.8
13	DahA[b]	-7.17	5887	14.0	13.2	13.3	14.2
14	BghiP[b]	-7.03	5834	13.9	13.1	13.2	14.1
15	IndP[b]	-7.00	5791	13.8	13.0	13.1	14.0

541 a: Harner and Bidleman (1998); b: Odabasi et al. (2006)
542
543
544
545
546
547
548
549
550

Table 2 Summary of particle-bound PAH concentrations (ng m^{-3}) in Lhasa and other regions

PAH	Ring	Mean(SD)	Minimum	Maximum	% of ΣPAHs	Reference
Ace	3	0.392 (0.079)	0.297	0.678	0.892	This study
Acel	3	0.405 (0.048)	0.330	0.536	0.922	,,
Ant	3	0.824 (0.298)	0.612	2.074	1.88	,,
Flu	3	0.742 (0.123)	0.545	1.01	1.69	,,
Phe	3	1.94 (2.17)	0.523	10.5	4.41	,,
BaA	4	4.26 (7.71)	0.556	39.9	9.70	,,
Chr	4	5.38 (8.10)	0.956	42.0	12.2	,,
Fla	4	6.71 (10.4)	0.501	55.7	15.3	,,
Pyr	4	6.51 (10.7)	0.865	57.2	14.8	,,
BaP	5	3.93 (5.96)	0.654	28.1	8.94	,,
BbF	5	5.59 (7.72)	0.887	21.6	9.48	,,
BkF	5	2.01 (3.72)	0.529	18.9	7.81	,,
DahA	5	0.849 (0.402)	0.582	2.29	1.93	,,
BghiP	6	2.30 (2.52)	0.710	12.1	5.24	,,
IndP	6	2.09 (2.64)	0.565	12.0	4.77	,,
Total PAHs		43.9 (54.6)	9.18	211	100	,,
Beijing[a]		148 (28)		-		Zhang et al., 2016
Delhi[b]		105	11.0	512		Sarkar and Khillare, 2013
Kathmandu[c]		155 (130)	18.1	453		Chen et al., 2015
Zhongba[c]		8.78 (4.50)	3.41	20.9		Chen et al., 2017
Nyalam[c]		5.57 (3.36)	3.62	16.9		Chen et al., 2017
Lulang[d]		0.59 (0.52)	0.06	2.53		Chen et al., 2014
Lhasa[e]		20 (15)	4.4	60		Liu et al., 2013
Lhasa[f]		35.7 (15.9)	11.4	72.5		Gong et al., 2011

a: 16 PAHs of TSP samples; b: 16 PAHs of PM_{10} samples; c: 15 PAHs of TSP samples; d: 17 PAHs of TSP samples; e: 15 PAHs of TSP samples; f: 22 PAHs of TSP samples.

581 Table 3 Calculated gas phase PAH concentrations in four seasons of Lhasa

582

SN	PAH	Spring	Summer	Autumn	Winter
1	Ace	506.2597	1528.076	448.5648	183.0286
2	Acel	893.5951	2440.036	732.5843	289.8921
3	Ant	80.33509	290.3747	82.25962	28.92283
4	Flu	497.3334	1239.61	681.354	562.8298
5	Phe	93.16859	335.6044	101.9659	37.49022
6	BaA	0.507878	0.912246	0.87494	0.523964
7	Chr	0.423029	0.867332	0.866197	0.493445
8	Fla	11.77585	22.81812	28.92497	19.83927
9	Pyr	17.74505	37.10413	31.53879	19.42907
10	BaP	0.013702	0.063772	0.064483	0.013267
11	BbF	0.013721	0.064625	0	0.010735
12	BkF	0.014141	0.047081	0.046888	0.017806
13	DahA	0.000416	0.002468	0.002228	0.000309
14	BghiP	0.000295	0.002407	0.000836	0.000104
15	IndP	0.000773	0.005072	0.00348	0.000478
	Total	2101.187	5895.588	2109.051	1142.492

583

584

585

586

587

588

589

590

591

592

593 Table 4 Diagnostic ratios of PAHs in Lhasa aerosols and their source profiles. Numbers in brackets
594 represent standard deviations
595

	Spring	Summer	Autumn	Winter	Source profiles	Reference
IndP/(IndP+BghiP)	0.44(0.03)	0.42(0.02)	0.47(0.03)	0.47(0.03)	<0.2 Petrogenic 0.2-0.5 Petroleum combustion >0.5 Coal and biomass	(Grimmer et al., 1983; Yunker et al., 2002)
Fla/(Fla+Pyr)	0.54(0.03)	0.48(0.02)	0.49(0.02)	0.52(0.03)	<0.4 Petrogenic 0.4-0.5 Petroleum combustion >0.5 Coal and biomass	(Bari et al., 2011; Sicre et al., 1987; Tang et al., 2005; Tsapakis and Stephanou, 2003)

596
597
598
599
600
601
602
603
604
605
606
607
608
609
610
611
612
613
614

615 Table 5 Values and probability distributions of parameters used in the exposure assessment

616

units	Children	Teens	Adults
Age (year)	0-10	11-20	21-70
IR[a] (m^3 day^{-1})	8.79	13.61	12.34
EF (day $year^{-1}$)	365	365	365
ED (year)	0-10	0-10	0-50
BW[b] (kg)	16.66	46.35	57.04
AT[a] (day)	25550	25550	25550
CFS[c] $(mg/(kg\ day))^{-1}$	3.14	3.14	3.14

617 a: cited from the US EPA; b: citied from statistical data from China; c: cited from Chen and Liao (2006).

618

619

620

621

622

623

624

625

626

627

628

629

630

631

632

633

634

635

Figure captions (in color online):

Fig. 1. Locations of sampling sites and the aerosol sampler (picture)

Fig. 2. Seasonal variations of PAH concentrations in Lhasa

Fig. 3. Seasonal variations of PAH compositions (three-, four-, five-, and six-ring PAHs) in Lhasa, number in bracket are sample sizes.

Fig. 4. PMF 5.0-generated factor profiles and their contributions to the 15 examined PAHs

Fig. 1

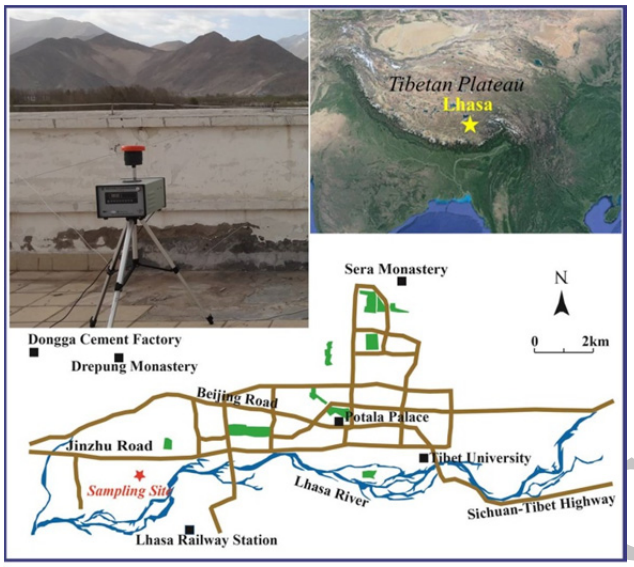

682 Fig. 2

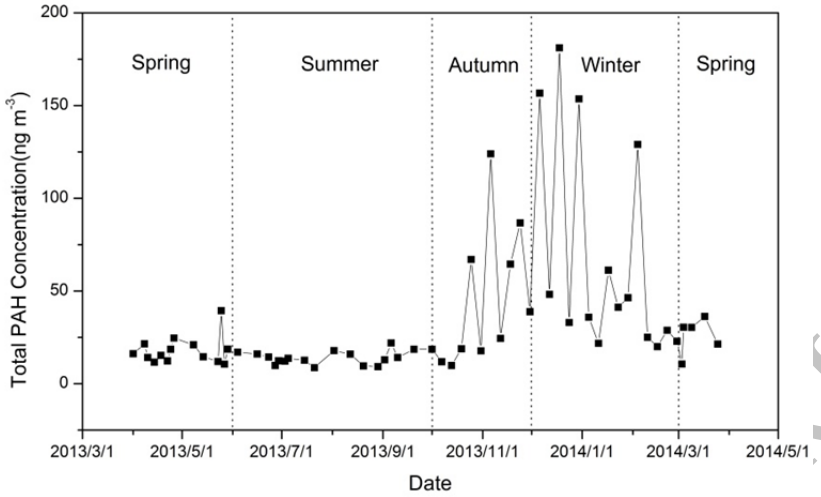

683
684
685
686
687
688
689
690
691
692
693
694
695
696
697
698
699
700
701
702
703

Fig. 3

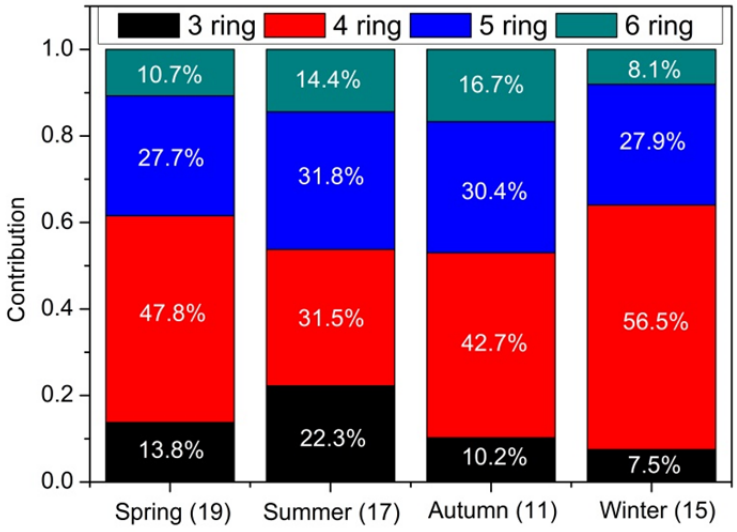

725 Fig. 4

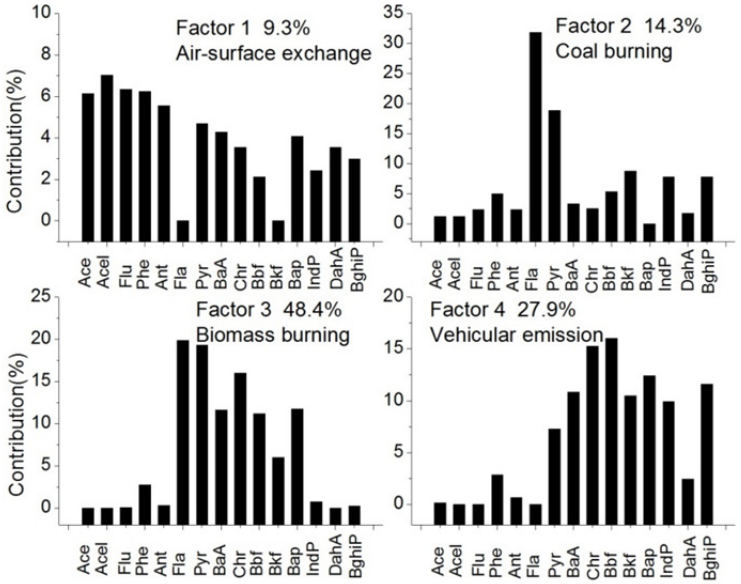

726

727